AUT Journal of Mechanical Engineering

AUT J. Mech. Eng., 5(3) (2021) 451-464
DOI: 10.22060/ajme.2021.18498.5902

Computational fluid dynamics modeling of effect of dipleg geometry on separation efficiency of a square cyclone

E. Fatahian, H. Fatahian*

Department of Mechanical Engineering, Nour Branch, Islamic Azad University, Nour, Iran

ABSTRACT: In the present work, an effective way is introduced to improve the efficiency of a square cyclone separator. For this aim, a dipleg is attached under the square cyclone to investigate its geometry effect on the performance of square cyclone separator. A three-dimensional computational fluid dynamics simulation is done by solving the Reynolds averaged Navier Stokes equations with the Reynolds stress model turbulence model and using the Eulerian-Lagrangian two phase method. The particle dispersion due to turbulence in the gas phase is predicted using the discrete random Walk model. The predicted results show that using a dipleg although produces an increase in pressure drop but it positively enhances the separation efficiency of the square cyclone. In the present results, the pressure drop is increased by about 19% by using dipleg at an inlet velocity of 28 m/s. Using dipleg significantly increases the separation efficiency of square cyclone especially at higher inlet velocity. This can be more obvious when using dipleg 1 which is minimized the 50% cut size of square cyclone by about 35.5%. Also, in higher inlet velocity, the reduction value of 50% cut size is higher which is proved that using dipleg is more effective due to stronger swirl flow.

Review History:

Received: Jun. 04, 2020
Revised: Nov. 26, 2020
Accepted: Dec. 24, 2020
Available Online: Jan. 22, 2021

Keywords:

Square cyclone
Pressure drop
Separation efficiency
Numerical simulation
Dipleg

1- Introduction

Generally, a cyclone separator is widely employed in the industrial process to remove the dust of gaseous flows [1]. They are applied in gas-solid separation and control air pollution for industrial applications. Cyclone is popular due to easy maintenances, low cost, easy operation, and reliability under extreme working conditions [2]. Their major factors of performance are collection and fractional efficiency, as well as pressure drop. Many works have been done in the domain of cyclone separators to specify their characteristics [3-5]. Zhao et al. [6] considered the performance of the cyclone and concluded that the cyclone separator using a spiral double inlet can increase the particle separation efficiency. Balestrin et al. [7] considered the effect of the vortex finder outlet duct as well as a stretched cylindrical body on the performance of a cyclone. They found that the efficiency of cyclone enhances with a secondary swirling flow promoted by decreasing in cross-section of the vortex finder. Safikhani et al. [8] numerically investigated the particle dynamics and fluid flow for determining the performance of a cyclone separator. They stated that the turbulent kinetic energy has high values at the entrance of the vortex finder. Generally, cyclones are divided into square and conventional ones. The conventional cyclone, which is commonly used in the CFB boiler, has a circular cross-section. In the progress of large CFB boilers, the huge body of the conventional cyclone became the main problem due to the thick refractory wall that needs a long period to start the boiler. Using a square can be an alternative and effective way to dominate this major shortcoming [9,10]. Because of shorter start-stop time and at the same time easy integration with the boiler, easier membrane wall arrangement, and convenient construction, the square cyclones have more advantages over conventional cyclones. Yue et al. [11] examined a square cyclone separator with a curved inlet and the designed square cyclone implemented in a CFB boiler in China [12,13]. Junfu et al. [14] investigated the performance of the square cyclone which was used in the CFB boiler and indicated that the pressure drop was less than 800 Pa. Huang et al. [15] enhanced the separation efficiency of a cyclone using the laminarizer and a better cyclone 50% cut size performance was obtained. Fatahian et al. [16], numerically investigated the effect of using the laminarizer on the characteristics of the conventional and the square cyclones. Their results demonstrated that using the laminarizer in the square cyclone was more effective. Moreover, Fatahian et al. [5], modified the conical section of a square cyclone with single-cone to dual inverse-cone shape which improves the separation efficiency of the square cyclone. Although many studies have been done for considering the impact of various geometric parameters on cyclone performance, there has been little work on the influence of dust outlet geometry such as dustbin and dipleg. Obermair et al. [17] examined various dust outlet geometries for finding the impact of dust outlet geometry on cyclone efficiency. Their study revealed that the efficiency of separation can be enhanced remarkably by modifying dust outlet

*Corresponding author's email: fatahianhossein@gmail.com

geometry. The effect of a dipleg was proposed and studied in some researches [18-23]. Qian et al. [24] investigated a cyclone prolonged with a dipleg numerically and experimentally. They concluded that a dipleg could improve separation efficiency remarkably.

Inspired by the previous studies, it is proved that the square cyclones generated lower separation efficiency compared to the conventional cylindrical cyclone. However, rare studies focused on developing new designs to improve the performance of the square cyclones. Hence, the main objective of the present study is to analyze the performance of cyclones focusing on proposing a new shape of a square cyclone to overcome the problem of low efficiency. In the present study, a dipleg is attached to the bottom of the square cyclone which could be an easier solution rather than modifying the whole cyclone to enhance the overall performance. Furthermore, no numerical study has been yet conducted to consider the effect of dipleg geometry on the performance of a square cyclone.

2- Geometry

Figs. 1 and 2 indicate the schematic views of a square cyclone without and with different shapes of dipleg. A dipleg is a device to carry solid particles from a gas-solid cyclone separator downward into a dustbin [22]. The geometrical dimensions of the base square cyclone (without dipleg) are considered for validation based on experimental data of Zheng et al. [25]. Moreover, the main geometrical dimensions of a square cyclone with dipleg are kept constant compared to without dipleg case and only the barrel height is modified. The geometrical dimensions for all cases are depicted in Table 1.

3- Governing Equations

In order to simulate the flow inside the square cyclone separator, the three-dimensional CFD simulation is conducted. The Reynolds-Averaged Navier–Stokes (RANS) equations for the steady and incompressible Newtonian flow can be written as follows [26]:

$$\frac{\partial \bar{u}_i}{\partial x_i} = 0 \qquad (1)$$

$$\frac{\partial \bar{u}_i}{\partial x_i} + \bar{u}_j \frac{\partial \bar{u}_i}{\partial x_j} = -\frac{1}{\rho}\frac{\partial \bar{P}}{\partial x_i} + \upsilon \frac{\partial^2 \bar{u}_i}{\partial x_j \partial x_j} - \frac{\partial}{\partial x_j} R_{ij} \qquad (2)$$

where $\bar{u}_i$ and x_i are the mean velocity and the position, respectively. ρ and ν denote the gas density and the gas kinematic viscosity, respectively. $\bar{P}$ is the mean pressure, $R_{ij} = \overline{u_i' u_j'}$ is the Reynolds stress tensor. Here $u_i' = u_i - \bar{u}_i$ is the i th fluctuating velocity component.

Due to the three dimensional and highly swirling (non-isotropic) flow in the cyclone separators, neither the standard k-ε, RNG k-ε nor Realizable k-ε turbulence models are capable of these types of flows [27-30]. Moreover, many researchers verified the ability of the Reynolds stress model (RSM) in modeling the cyclonic flow (e.g., [31-35]). The Reynolds stress turbulence model (RSM) [36] has been adopted in the present simulation to predict the turbulent flow in the square cyclone.

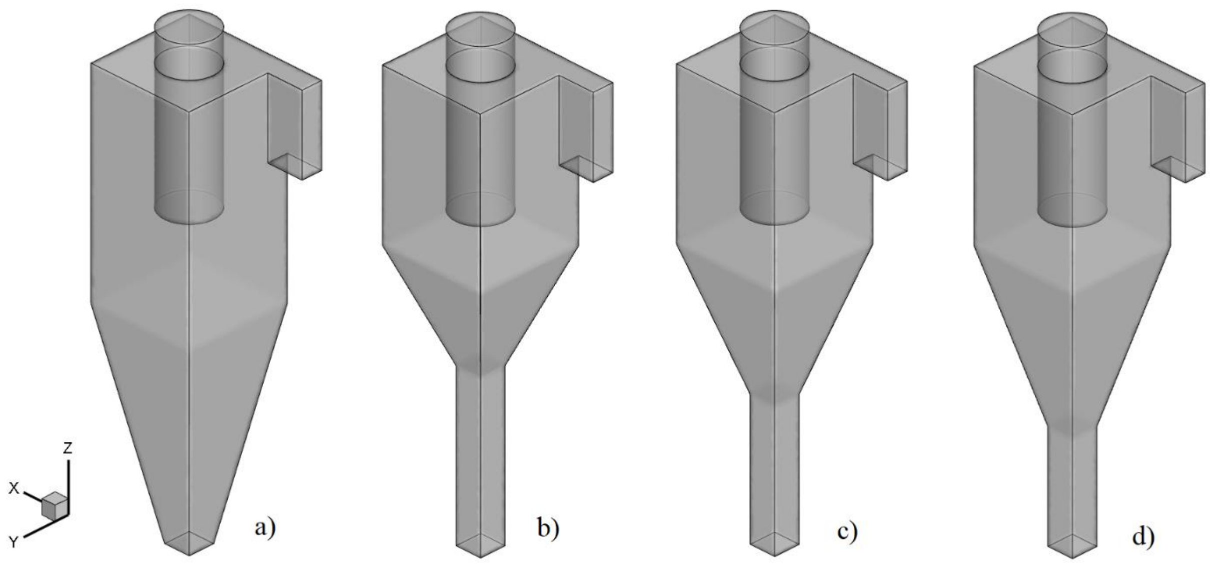

Fig. 1. Schematic view of a square cyclone a) without dipleg b) with dipleg 1 c) with dipleg 2 d) with dipleg 3

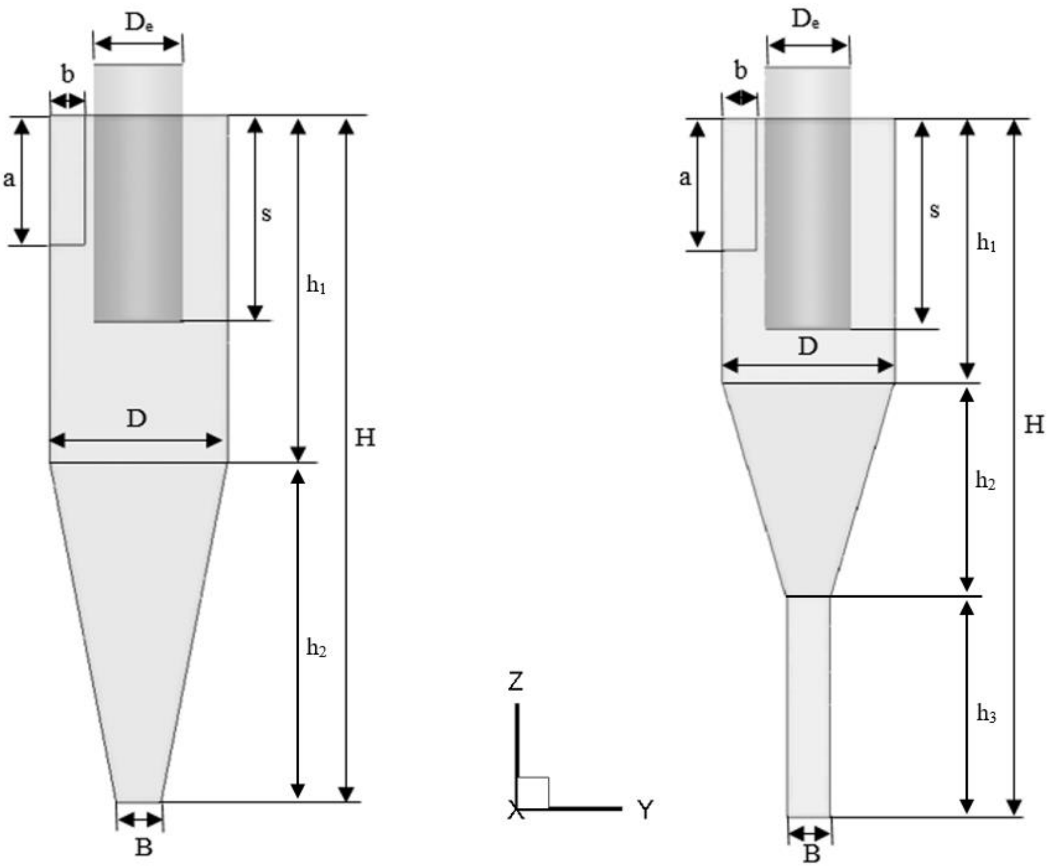

Fig. 2. Geometrical dimensions of square cyclone without dipleg (left) and with dipleg (right)

Table 1. Details of geometrical dimensions of square cyclones (D=200 mm)

Dimensions	*a/D*	*b/D*	D_e/D	*S/D*	h_1/D	h_2/D	*h3/D*	*H/D*	*B/D*
Without dipleg	0.75	0.2	0.5	1.2	2	2	-	4	0.25
With dipleg 1	0.75	0.2	0.5	1.2	1.5	1	1.5	4	0.25
With dipleg 2	0.75	0.2	0.5	1.2	1.5	1.25	1.25	4	0.25
With dipleg 3	0.75	0.2	0.5	1.2	1.5	1.5	1	4	0.25

The RSM turbulence model provides differential transport equations to evaluate the turbulence stress components:

$$\frac{\partial}{\partial t} R_{ij} + \bar{u}_k \frac{\partial}{\partial x_k} Rij = \frac{\partial}{\partial x_k}\left(\frac{v_t}{\partial^k}\frac{\partial}{\partial x_k} R_{ij}\right) - \left[R_{ik}\frac{\partial \bar{u}_j}{\partial x_k} + R_{jk}\frac{\partial \bar{u}_k}{\partial x_k}\right] - C_1\frac{\varepsilon}{K}\left[R_{ij} - \frac{2}{3}\delta_{ij}K\right] - C_2\left[P_{ij} - \frac{2}{3}\delta_{ij}P\right] - \frac{2}{3}\delta_{ij}\varepsilon \quad (3)$$

where the turbulence production terms P_{ij} are expressed as [37]:

$$P_{ij} = -\left[R_{ik}\frac{\partial \bar{u}_j}{\partial x_k} + R_{jk}\frac{\partial \bar{u}_k}{\partial x_k}\right], P = \frac{1}{2}P_{ij} \quad (4)$$

with P being the fluctuating energy production, v_t is the turbulent (eddy) viscosity; and $\sigma^k = 1$, $C_1 = 1.8$, $C_2 = 0.6$ are empirical constants. The transport equation for turbulence dissipation rate, ε, is defined as [38]:

$$\frac{\partial \varepsilon}{\partial t} + \partial \bar{u}_j \frac{\partial \varepsilon}{\partial x_j} = \frac{\partial}{\partial x_j}\left(v + \frac{v_t}{\partial^k}\frac{\partial}{\partial x_j}\right) - C^{\varepsilon 1}\frac{\varepsilon}{K}R_{ij}\frac{\partial \bar{u}_i}{\partial x_j} - C^{\varepsilon 2}\frac{\varepsilon^2}{K} \quad (5)$$

In Eq. (5), $K = \frac{1}{2}\overline{u_i^{'}u_i^{'}}$ is the fluctuating kinetic energy, and ε is the turbulence dissipation rate. The values of constants are $\sigma^{\varepsilon} = 1.3$, $C^{\varepsilon 1} = 1.44$, $C^{\varepsilon 2} = 1.92$.

In this study, the one-way coupling method is applied for solving two-phase flow and the Eulerian-Lagrangian approach is carried out to simulate the second discrete phase (particles). Moreover, the prediction of particle tracking in the cyclone and the calculation of collection efficiency are done using a discrete phase model (DPM) method with neglecting particle-particle interactions [39]. In this model, individual particles are tracked through the continuum fluid [34]. The drag coefficient for spherical particles calculated according to Morsi and Alexander method [40]. Furthermore, the particle dispersion due to turbulence in the gas phase is predicted using the discrete random walk (DRW) model [16,41].

The equation of particle motion is defined as [42]:

$$\frac{du_{pi}}{dt} = \frac{18\mu}{\rho_p d_p^2}\frac{C_D \mathrm{Re}_p}{24}\left(u_i - u_{pi}\right) + \frac{g_i\left(\rho_p - \rho\right)}{\rho_p} \quad (6)$$

$$\frac{dx_{pi}}{dt} = u_{pi} \quad (7)$$

ρ_p and d_p are the particle density and diameter respectively, C_D represents the drag coefficient, u_i and u_{pi} are the gas and particle velocity in i direction respectively. μ and ρ denote the dynamic viscosity and gas density respectively. g_i represents the gravitational acceleration in i direction and Re_p denotes the relative Reynolds number.

$$\mathrm{Re}_p = \frac{\rho_p D_p \left|u - u_p\right|}{\mu} \quad (8)$$

Numerical setting

The gas phase is treated as air with a constant density of 1.225 kg/m^3 and a viscosity of 1.7894×10^{-5} kg/ms. The particle density is 1989.7 kg/m^3 with an inlet concentration of 8.8 g/m^3 and the particle size varies from 1 to 32 µm. The boundary condition at the gas inlet section is set as inlet velocity and it is supposed that the inlet velocities of particles and gas are equal. Turbulence intensity is chosen to be 5% [31,43,44]. The outflow condition is set for the gas outlet section. Moreover, no-slip wall condition is set for cyclone walls, and trap DPM condition is used at the bottom of the cyclone body. ANSYS Fluent 18.2 CFD code is implemented to solve Navier-Stokes equations in conjunction with the RSM and the standard wall function according to the strong swirl flow in the cyclone to consider the effect of turbulence. The numerical settings of the CFD simulation are presented in Table 2.

1. Grid Independence Study and Validation

In the present study, four structured hexahedral cells are used to verify the independence of CFD results which are illustrated in Fig. 3. Four different cell numbers of 193483, 354872, 518124, and 677372 are employed for the computational domain to investigate the grid independency. The radial profiles for the static pressure of square cyclone without a dipleg are shown in Fig. 4. The cell number 518124 is chosen as the optimum cells for the square cyclone without a dipleg. A similar grid independence study is performed for the square cyclone with a dipleg which the cell number 547098 is selected as the optimum cell.

Table 2. Numerical settings of the present CFD simulation

Model conditions	Model settings
Flow regime	Steady-state
Turbulence	Reynolds stress model (RSM)
Solution method	Pressure-velocity coupling: SIMPLEC
Spatial discretization:	Pressure: PRESTO!
	Momentum: Quick
	Turbulent kinetic energy: Second-order upwind
	Specific dissipation rate: Second-order upwind
	Reynolds stresses: First-order upwind
Convergence criteria	For all equations is set as 10^{-5}

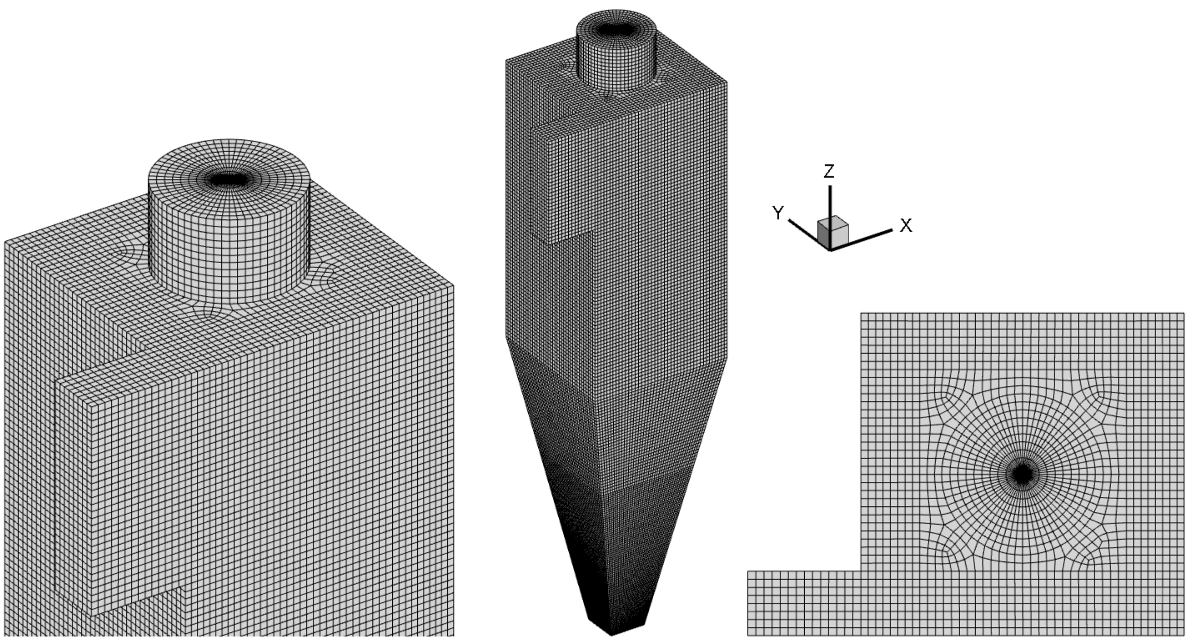

Fig. 3. Computational grids for the base square cyclone

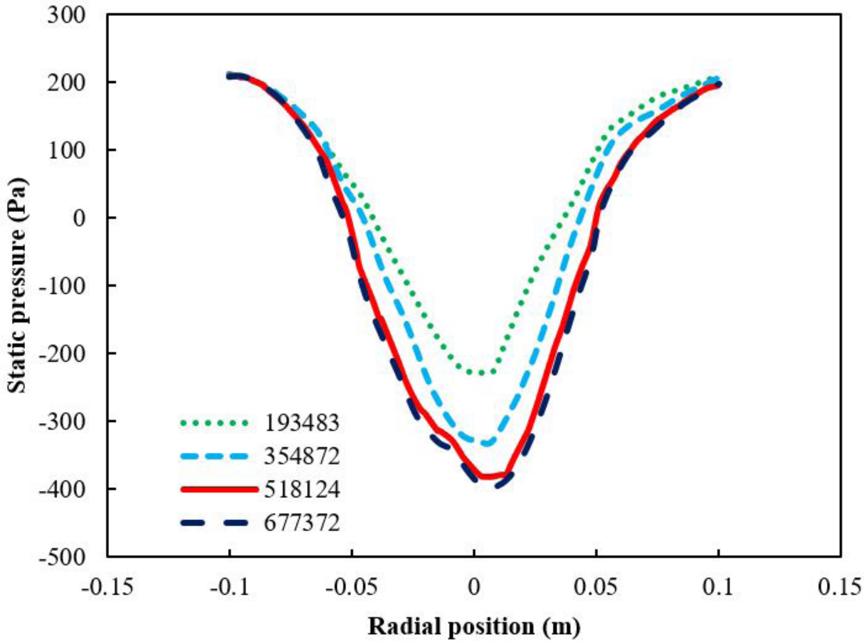

Fig. 4. The radial profiles for the static pressure of square cyclone without dipleg at y=0.15 m for different cell numbers at an inlet velocity of 20 m/s

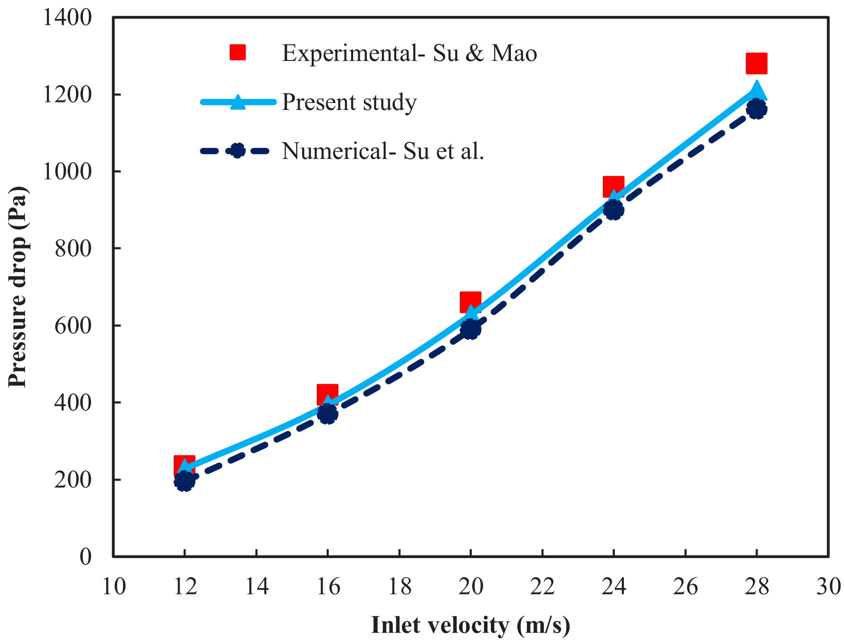

Fig. 5. Comparison between the pressure drop of the present study and experimental data [25] and numerical results [9]

As shown in Figs. 5 and 6, the results are verified by comparing them with the experimental data of Zheng et al. [25], numerical results done by Su et al. [9], and the Lapple model [45]. The difference between static pressure at the cyclone inlet section and outlet section is defined as the pressure drop, which can measure the energy loss of cyclone. It is obvious that the pressure drop is nonlinearly increased with the increment of inlet velocity. Energy loss increases as the inlet velocity increases. A comparison of both pressure drop and separation efficiency demonstrates that the CFD results agreed well with literature results while the maximum error between them was about 5%.

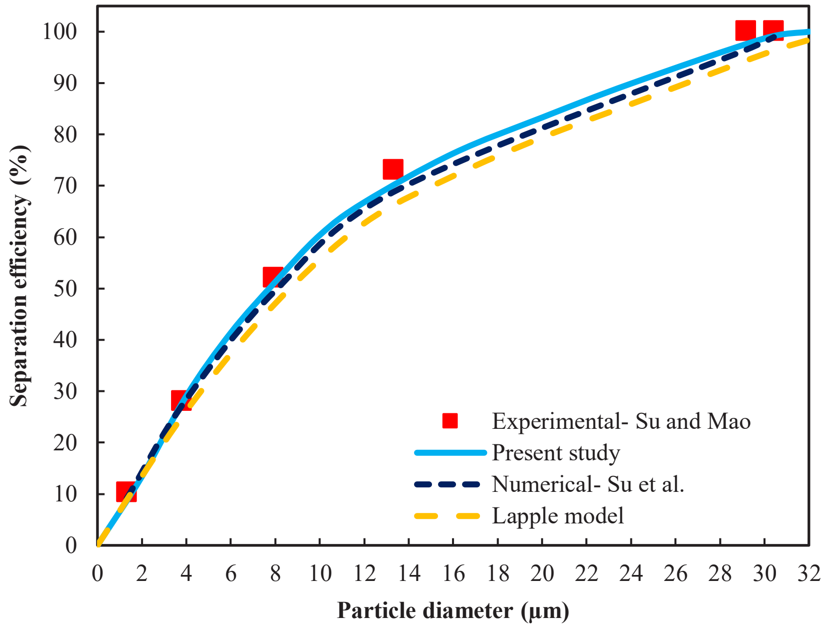

Fig. 6. Comparison between the separation efficiency of the present study and experimental data [25], numerical results [9], and the Lapple model [45] at v=20 m/s

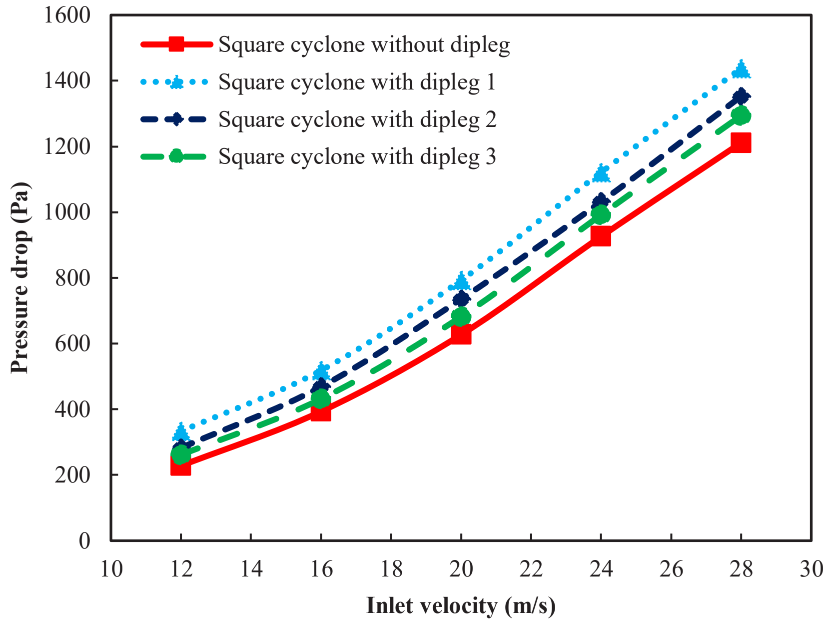

Fig. 7. The effect of inlet velocity on the pressure drop

4- Results and Discussion

In the numerical simulation, the inlet velocity of the cyclone is varied from 12 to 28 m/s to be consistent with the experimental study of Zheng et al. [25]. Pressure drop is one of the important parameters in designing a cyclone as it is correlated to the energy which cyclone employs. The cyclone pressure drop can be defined as the difference between the inlet pressure and outlet pressure [16]. The pressure drop values are obtained for the square cyclone separator with and without dipleg as shown in Fig. 7. It is observed that the pressure drop slightly increased with increasing inlet velocity [16,39]. Using a dipleg caused a considerable increase in pressure drop because of the energy dissipation by the stronger turbulent swirling flow across the cyclone. This is more evident in higher inlet velocity, especially at v=28 m/s. In this velocity, using dipleg 1 increased the pressure drop by about 19% compared to cyclone without dipleg. This can be clarified by the reduction of wall friction in the cyclone since less dust is re-entrained from the dipleg zone into the cyclone [24].

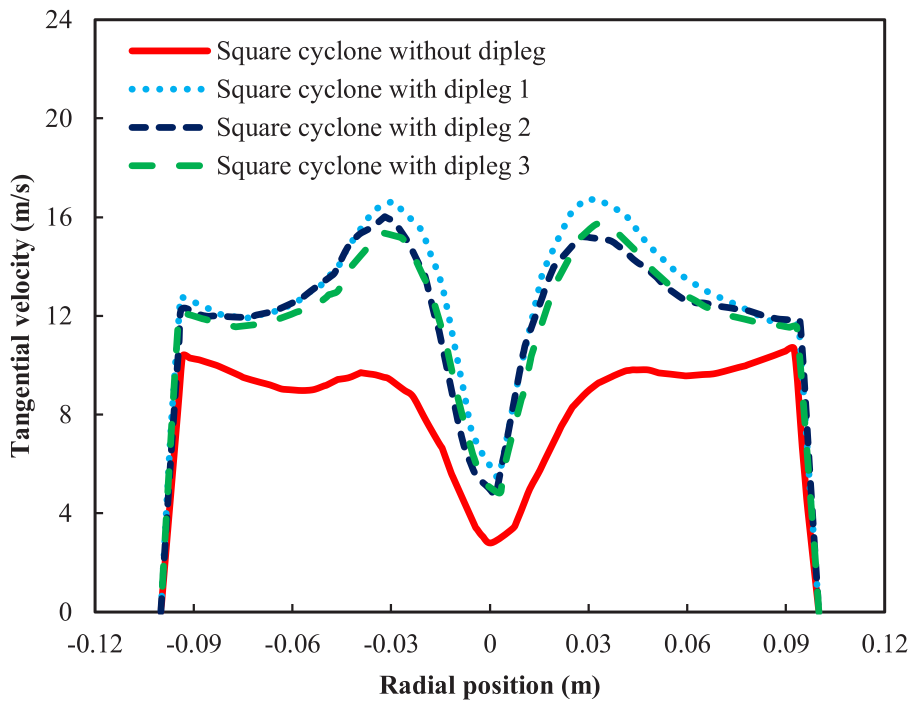

Fig. 8. Comparison of tangential velocity distribution at location y=0.15 m and v=12 m/s

The effect of dipleg on the distribution of the tangential velocity at y = 0.15 m (below the vortex finder) is shown in Fig. 8 at an inlet velocity of 12 m/s. A free vortex in the outer region and a forced vortex at its inner part (V-shaped) were observed for both cyclones which presented the expected Rankine-type vortex [46]. The tangential velocity is approximately distributed symmetrically around the central axis of the square cyclones. Furthermore, the maximum tangential velocity was observed in the region between the inner and outer vortexes [47]. The results demonstrated that using a dipleg influenced the distribution of the tangential velocity. It can be seen that the tangential velocity profiles varied significantly in the free and forced vortex regions, while the tangential velocity profiles remained approximately unchanged near the wall. Comparing the tangential velocity profiles for all square cyclones with dipleg revealed that square cyclone with dipleg 1 produced the maximum tangential velocity among all square cyclones due to smaller separation zone. The maximum tangential velocity was obtained about 1.4 times of the inlet velocity for square cyclone with dipleg 1, while it was predicted 0.89 times of the inlet velocity for square cyclone without dipleg. It can be concluded that the cyclone with dipleg produced higher values of tangential velocity compared to the cyclone without dipleg. This indicated that the square cyclone using dipleg was capable to increase the tangential velocity resulted in a significant increment of separation efficiency.

Figs. 9 and 10 show the comparison between separation efficiencies of the square cyclone separator with and without dipleg at two inlet velocities of 12 and 20 m/s as a function of particle diameter (in µm), respectively. The separation efficiency is calculated by tracking the released particles from the entrance section of the square cyclone which is done by utilizing the DPM model. The particle diameter varies in a wide range from 1 to 32 µm. A comparison of these figures proved that the separation efficiency is increased by increasing inlet velocity for the square cyclone with and without dipleg. Using a dipleg significantly improved the separation efficiency of square cyclones especially at higher inlet velocity. Comparing all cases has proved the fact that the separation efficiency of the square cyclone with dipleg 1 is higher than other cyclones. This is due to stronger swirl flow across the square cyclone with dipleg compared to the square cyclone without dipleg in the same inlet velocity.

The effect of dipleg geometry on 50% cut sizes for different inlet velocities is demonstrated in Table 3 which are extracted from the curves of separation efficiency. The particle size for which cyclone collection efficiency is 50% is defined as the 50% cut size [39]. It is found that the 50% cut size decreased by any increase of inlet velocity which is reported in the literature [16,39]. Using a dipleg positively enhanced the 50% cut size and consequently decreased it for all inlet velocities. Comparing the values of 50% cut sizes at each inlet velocity confirms that using dipleg is more effective in higher inlet velocities. Using dipleg 1 reduced the 50% cut size by about 20% and 35.5% for inlet velocities of 12 m/s and 28 m/s, respectively.

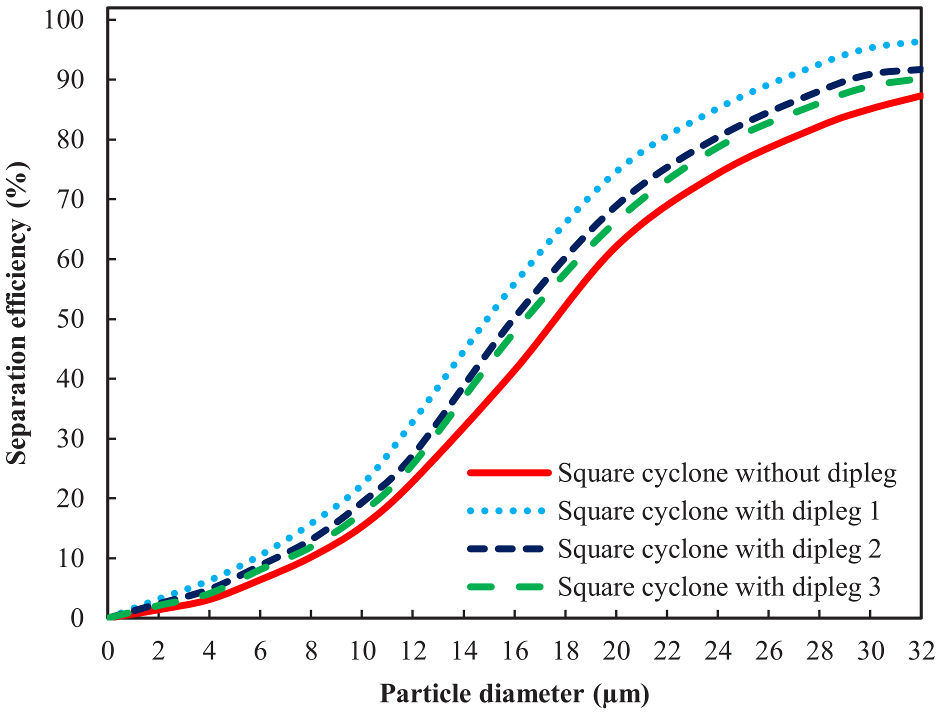

Fig. 9. Comparison between the separation efficiency of a square cyclone with and without dipleg at v=12 m/s

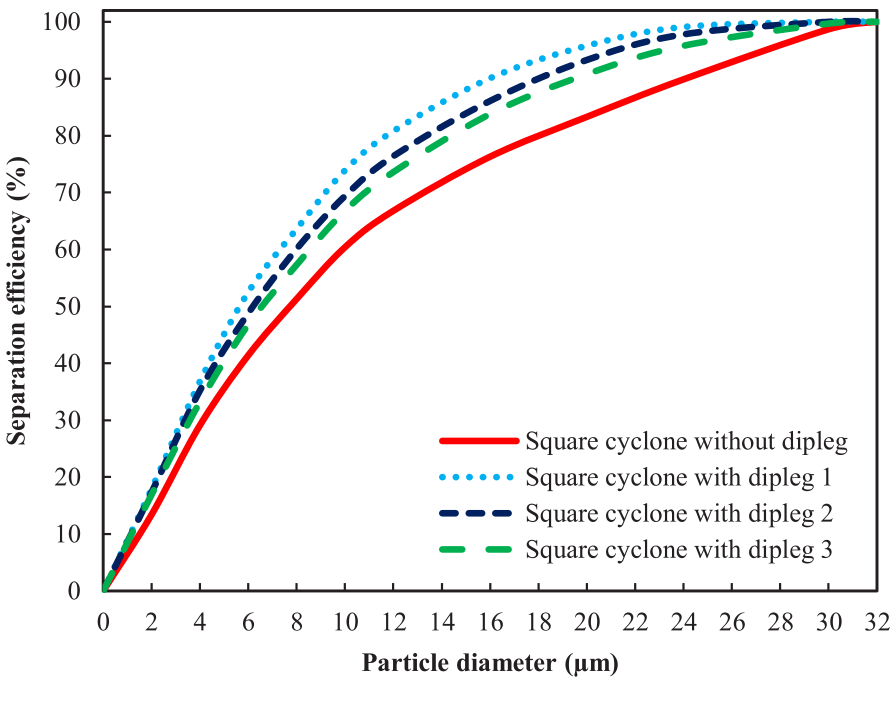

Fig. 10. Comparison between the separation efficiency of a square cyclone with and without dipleg at v=20 m/s

Table 3. Comparison of the 50% cut sizes (μm)

Inlet velocity (m/s)	12	16	20	24	28
Square cyclone without dipleg	17.67	12.27	7.94	5.21	3.91
Square cyclone with dipleg 1	14.16	9.89	5.87	3.42	2.52
Square cyclone with dipleg 2	15.82	10.41	6.29	4.02	2.88
Square cyclone with dipleg 3	15.94	10.74	6.76	4.29	3.02

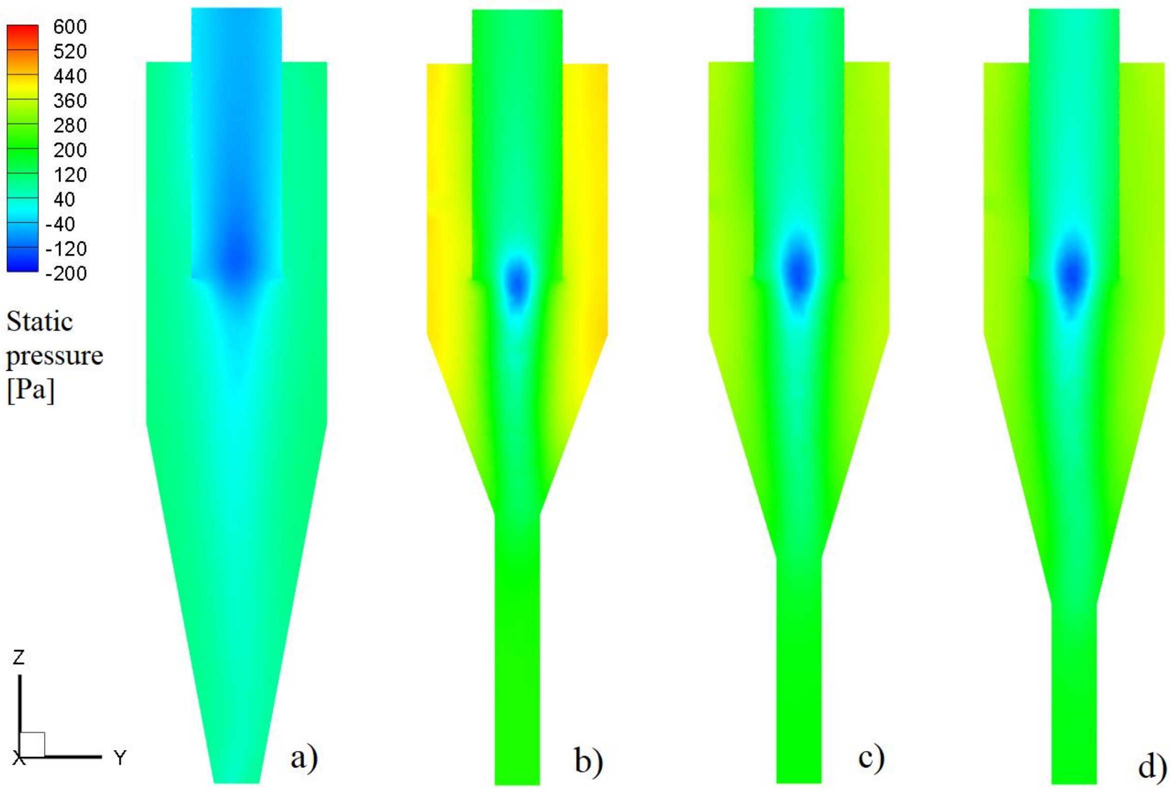

Fig. 11. Contours of static pressure for square cyclone a) without dipleg b) with dipleg 1 c) with dipleg 2 d) with dipleg 3 at v=12 m/s

Fig. 11 indicates the static pressure distribution in the square cyclone separator with and without dipleg for inlet velocity of 12 m/s. In the central zone, a negative pressure zone is observed due to the swirling velocity [39]. The lowest value of static pressure has appeared inside the vortex finder. Clearly, the static pressure is reduced radially from wall to center. The pressure gradient is large along the radial direction, as there is a highly intensified forced vortex [48]. In fact, near the cyclone wall, the positive values and maximum pressure are obtained while the lowest values are obtained near

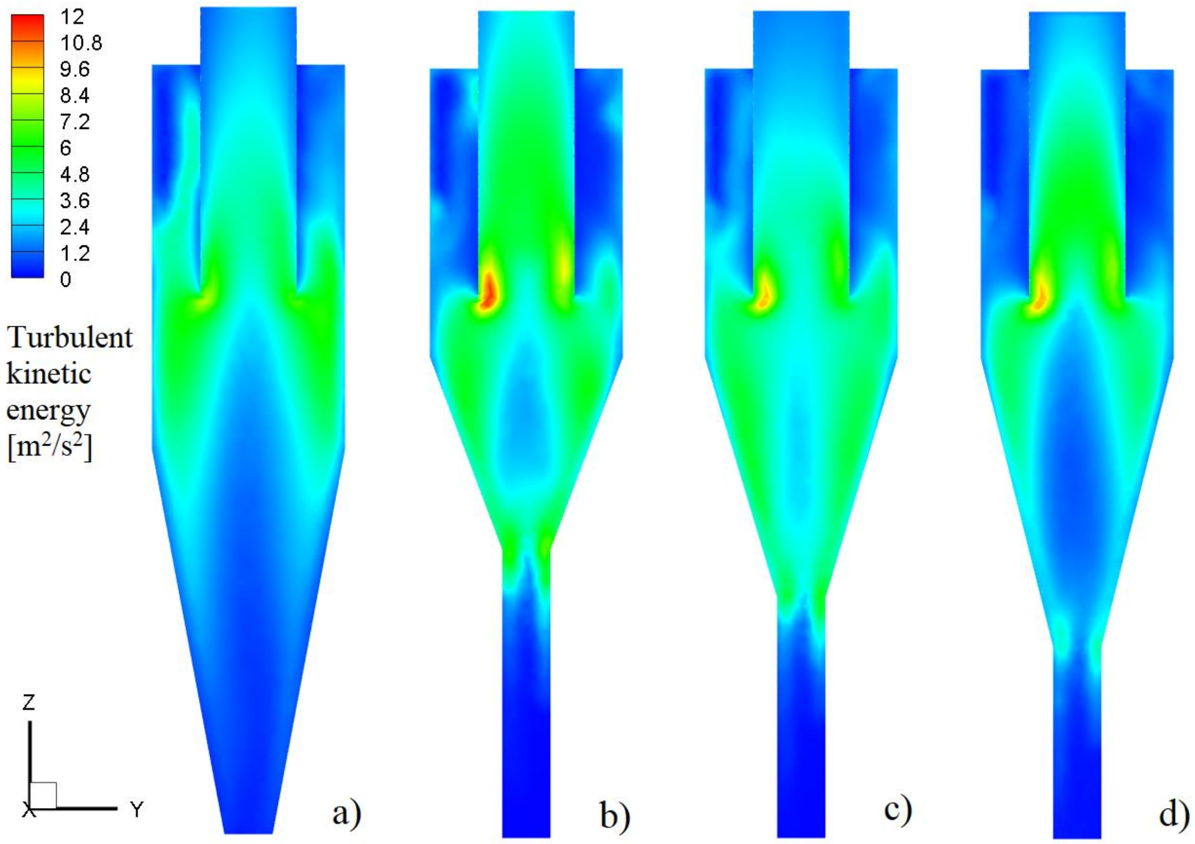

Fig. 12. Contours of turbulent kinetic energy for square cyclone a) without dipleg b) with dipleg 1 c) with dipleg 2 d) with dipleg 3 at v=12 m/s

the cyclone center. Obviously, all diplegs increased the static pressure, especially near the cyclone wall. The maximum increment of static pressure was seen in the square cyclone with dipleg 1. In Fig. 12, the effect of dipleg geometry on turbulent kinetic energy distribution is illustrated for the inlet velocity of 12 m/s. It is shown that the highest values of the turbulent kinetic are observed in the center near the entrance section of the vortex finder. Also, the forced vortex and free vortex regions are obtained in the center and periphery of the square cyclone, respectively, while the turbulent kinetic energy of square cyclone with dipleg near the entrance section of vortex finder is higher than that in the square cyclone without dipleg which can overcome the adverse pressure gradient. Moreover, when the dipleg is attached under the square cyclone, a low region of turbulent kinetic energy has appeared which prevented the entrainment of particles and enhanced the separation efficiency.

Fig. 13 presents the velocity vector in the square cyclone separator with and without dipleg for inlet velocity of 12 m/s. The flow is downward near the walls, while the flow is upward in the center zone at bottom of the vortex finder. The downward flow forced the particles to transport to the cone and dustbin, while the reversed flow may re-entrain some of the particles and drag them to escape into the gas outlet section. Increasing the slope of cone and using dipleg affected more on the downward flow. It can be seen the downward flow is accelerated in cyclone with dipleg 1 which experiences a higher centrifugal force among all cyclones. This is favorable for particle separation. Furthermore, lower velocity magnitude at dipleg section prevented the re-entrainment of particles from the lower part of dipleg to the main body of the cyclone.

5- Conclusions

In the present study, a dipleg is attached to the bottom of the square cyclone which could be an easier solution rather than modifying the whole cyclone to enhance its performance. A 3-D CFD analysis is done to consider the effect of dipleg geometry on the performance of a square cyclone.

The CFD results can be summarized as:

- It is concluded that the separation efficiency improved by using a dipleg which affected the flow pattern.
- It is observed that the pressure drop is increased slightly with increasing inlet velocity.
- The pressure drop is increased by about 19% by using dipleg at an inlet velocity of 28 m/s.

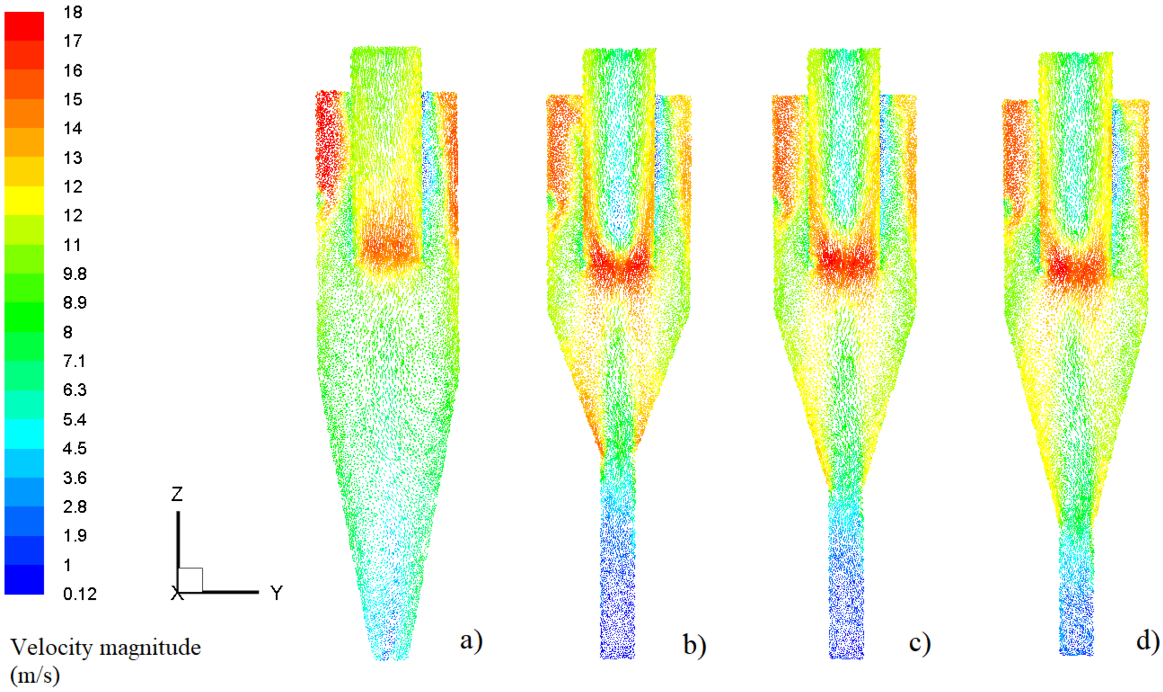

Fig. 13. Velocity vector for square cyclone a) without dipleg b) with dipleg 1 c) with dipleg 2 d) with dipleg 3 at v=12 m/s

- The 50% cut size is reduced when a dipleg is used under square cyclone for all inlet velocities.
- In higher inlet velocity, the reduction value of 50% cut size is higher which is proved that using dipleg is more effective due to stronger swirl flow.
- Using a dipleg reduces the 50% cut size by about 20% and 35.5% for inlet velocities of 12 m/s and 28 m/s, respectively.
- The thermophysical properties of gas change with temperature. Therefore, the performance of cyclones depends on the temperature of the operating fluid. The separation efficiency of square cyclone decreases with increasing inlet temperature. This obviously needs further investigation in future works.

References

[1] W. P. Martignoni, S. Bernardo, C. L. Quintani, Evaluation of cyclone geometry and its influence on performance parameters by computational fluid dynamics (CFD), Brazilian journal of chemical engineering, 24(1) (2007) 83-94.

[2] F. Zhou, G. Sun, X. Han, Y. Zhang, W. Bi, Experimental and CFD study on effects of spiral guide vanes on cyclone performance, Advanced Powder Technology, 29(12) (2018) 3394-3403.

[3] A. C. Hoffmann, M. De Groot, W. Peng, H. W. Dries, J. Kater, Advantages and risks in increasing cyclone separator length, AIChE journal, 47(11) (2001) 2452-2460.

[4] M. Shin, H. Kim, D. Jang, J. Chung, M. Bohnet, A numerical and experimental study on a high efficiency cyclone dust separator for high temperature and pressurized environments, Applied Thermal Engineering, 25(11) (2005) 1821-1835.

[5] H. Fatahian, E. Hosseini, E. Fatahian, CFD simulation of a novel design of square cyclone with dual-inverse cone, Advanced Powder Technology, 31(4) (2020) 1748-1758.

[6] B. Zhao, Y. Su, J. Zhang, Simulation of gas flow pattern and separation efficiency in cyclone with conventional single and spiral double inlet configuration, Chemical Engineering Research and Design, 84(12) (2006) 1158-1165.

[7] E. Balestrin, R. Decker, D. Noriler, J. Bastos, H, Meier, An alternative for the collection of small particles in cyclones: Experimental analysis and CFD modeling, Separation and Purification Technology, 184 (2017) 54-65.

[8] H. Safikhani, P. Mehrabian, Numerical study of flow field in new cyclone separators, Advanced Powder Technology, 27(2) (2016) 379-387.

[9] Y. Su, A. Zheng, B. Zhao, Numerical simulation of effect of inlet configuration on square cyclone separator performance, Powder technology, 210(3) (2011) 293-303.

[10] S. Wang, M. Fang, Z. Luo, X. Li, M. Ni, K. Cen, Instantaneous separation model of a square cyclone, Powder Technology, 102(1) (1999) 65-70.

[11] G. Yue, X. Y. Zhang, Y. Li, The water cooled square separator with an acceleration inlet, Chinese Patent, No. 93235842 (1995) 2-15.

[12] L. Jun-Fu, G.Yue, Q. Liu, The design and operation of 75 t/h circulating fluidized bed boiler with water cooled separator, Chinese Electrical Power, 32(4) (1999) 61-75.

[13] J. Li, G.Yue, Q. Liu, The operation experience of a 130 t/h circulating fluidized bed boiler with water cooled square cyclone, Chinese Electrical Power, 32(4) (2001) 19-33.

[14] L. Junfu, Z. Jiansheng, Z. Hai, L. Qing, Y. Guangxi, Performance evaluation of a 220t/h CFB boiler with water-cooled square cyclones, Fuel processing technology, 88(2) (2007) 129-135.

[15] A. Huang, N, Maeda, D. Shibata, T. Fukasawa, H. Yoshida, H. Kuo, K. Fukui, Influence of a laminarizer at the inlet on the classification performance of a cyclone separator, Separation and Purification Technology, 174 (2017) 408-416.

[16] H. Fatahian, E. Fatahian, M. E. Nimvari, Improving efficiency of conventional and square cyclones using different configurations of the laminarizer, Powder technology, 339 (2018) 232-243.

[17] S. Obermair, J. Woisetschläger, G. Staudinger, Investigation of the flow pattern in different dust outlet geometries of a gas cyclone by laser Doppler anemometry, Powder Technology, 138(2) (2003) 239-251.

[18] A. C. Hoffmann, M. De Groot, A. Hospers, The effect of the dust collection system on the flowpattern and separation efficiency of a gas cyclone, The Canadian Journal of Chemical Engineering, 74(4) (1996) 464-470.

[19] C. Cortes, A. Gil, Modeling the gas and particle flow inside cyclone separators, Progress in energy and combustion Science, 33(5) (2007) 409-452.

[20] . Gil, C. Cortes, L. Romeo, J. Velilla, Gas-particle flow inside cyclone diplegs with pneumatic extraction, Powder Technology, 128(1) (2002) 78-91.

[21] K. Elsayed, C. Lacor, The effect of the dust outlet geometry on the performance and hydrodynamics of gas cyclones, Computers & Fluids, 68 (2012) 134-147.

[22] J. Wang, J. Bouma, H. Dries, An experimental study of cyclone dipleg flow in fluidized catalytic cracking, Powder technology, 112(3) (2000) 221-228.

[23] S. Kim, J. Lee, J. Koh, G. Kim, S. Choi, I. Yoo, Formation and characterization of deposits in cyclone dipleg of a commercial residue fluid catalytic cracking reactor, Industrial & Engineering Chemistry Research, 51(43) (2012) 14279-14288.

[24] F. Qian, J. Zhang, M. Zhang, Effects of the prolonged vertical tube on the separation performance of a cyclone, Journal of hazardous materials, 136(3) (2006) 822-829.

[25] A. Zheng, Y. Su, X. Wan, Experimental study of a square-shaped separator with different inlet forms, Journal of Engineering Thermal Energy Power, 23 (2008) 293-297.

[26] H. Safikhani, M. Akhavan-Behabadi, M. Shams, M. Rahimyan, Numerical simulation of flow field in three types of standard cyclone separators, Advanced Powder Technology, 21(4) (2010) 435-442.

[27] F. Kaya, I. Karagoz, A. Avci, Effects of surface roughness on the performance of tangential inlet cyclone separators, Aerosol science and technology, 45(8) (2011) 988-995.

[28] I. Karagoz, F. Kaya, CFD investigation of the flow and heat transfer characteristics in a tangential inlet cyclone, International Communications in Heat and Mass Transfer, 34(9) (2007) 1119-1126.

[29] T. Chuah, J. Gimbun, T. Choong, A CFD study of the effect of cone dimensions on sampling aero-cyclones performance and hydrodynamics, Powder technology, 162(2) (2006) 126-132.

[30] G. Wan, G. Sun, X. Xue, M. Shi, Solids concentration simulation of different size particles in a cyclone separator, Powder Technology, 183(1) (2008) 94-104.

[31] K. Elsayed, C. Lacor, Optimization of the cyclone separator geometry for minimum pressure drop using mathematical models and CFD simulations, Chemical Engineering Science, 65(22) (2010) 6048-6058.

[32] H. Fatahian, E. Fatahian, M. E. Nimvari, G. Ahmadi, Novel designs for square cyclone using rounded corner and double-inverted cones shapes, Powder Technology, 380 (2020) 67-79.

[33] L. Huang, K. Kumar, A. S. Mujumdar, Simulation of a spray dryer fitted with a rotary disk atomizer using a three-dimensional computational fluid dynamic model, Drying Technology, 22(6) (2004) 1489-1515.

[34] M. Azadi, M. Azadi, A. Mohebbi, A CFD study of the effect of cyclone size on its performance parameters, Journal of hazardous materials, 182(1) (2010) 835-841.

[35] K. Elsayed, C. Lacor, Modeling and Pareto optimization of gas cyclone separator performance using RBF type artificial neural networks and genetic algorithms, Powder Technology, 217 (2012) 84-99.

[36] B. Launder, G. Reece, W. Rodi, Progress in the development of a Reynolds-stress turbulence closure, Journal of fluid mechanics, 68(3) (1975) 537-566.

[37] S. Wang, M. Fang, Z. Luo, X. Li, M. Ni, K. Cen, Instantaneous separation model of a square cyclone, Powder Technology, 102(1) (1999) 65-70.

[38] A. Hoekstra, J. J. Derksen, H. E. A. Van Den Akker, An experimental and numerical study of turbulent swirling flow in gas cyclones, Chemical Engineering Science, 54(13) (1999) 2055-2065.

[39] H. Erol, O. Turgut, R. Unal, Experimental and numerical study of Stairmand cyclone separators: a comparison of the results of small-scale and large-scale cyclones, Heat and Mass Transfer (2019) 1-14.

[40] S. Morsi, A. J. Alexander, An investigation of particle trajectories in two-phase flow systems, Journal of Fluid mechanics, 55(2) (1972) 193-208.

[41] A. Raoufi, M. Shams, M. Farzaneh, R. Ebrahimi, Numerical simulation and optimization of fluid flow in cyclone vortex finder, Chemical Engineering and Processing: Process Intensification, 47(1) (2008) 128-

137.

[42] B. Zhao, Y. Su, J. Zhang, Simulation of gas flow pattern and separation efficiency in cyclone with conventional single and spiral double inlet configuration, Chemical Engineering Research and Design, 84(12) (2006) 1158-1165.

[43] S. Shukla, P. Shukla, P. Ghosh, Evaluation of numerical schemes for dispersed phase modeling of cyclone separators, Engineering Applications of Computational Fluid Mechanics, 5.(2) (2011) 235-246.

[44] T. Mothilal, K. Pitchandi, Influence of inlet velocity of air and solid particle feed rate on holdup mass and heat transfer characteristics in cyclone heat exchanger, Journal of Mechanical Science and Technology, 29(10) (2015) 4509-4518.

[45] C. B. Shephered, C. E. Lapple, Flow pattern and pressure drop in cyclone dust collectors, Industrial & Engineering Chemistry, 31(8) (1939) 972-984.

[46] S. Wang, H. Li, R. Wang, X. Wang, R. Tian, Q. Sun, Effect of the inlet angle on the performance of a cyclone separator using CFD-DEM, Advanced Powder Technology, 30(2) (2019) 227-239.

[47] Z. Liu, J. Jiao, Y. Zheng, Q. Zhang, L. Jia, Investigation of turbulence characteristics in a gas cyclone by stereoscopic PIV, AIChE journal, 52(12) (2006) 4150-4160.

[48] A. Raoufi, M. Shams, H. Kanani, CFD analysis of flow field in square cyclones, Powder Technology, 191(3) (2009) 349-357.

HOW TO CITE THIS ARTICLE

E. Fatahian, H. Fatahian, Computational fluid dynamics modeling of effect of dipleg geometry on separation efficiency of a square cyclone. AUT J. Mech Eng., 5(3) (2021) 451-464.

DOI: 10.22060/ajme.2021.18498.5902